The Journal of Immunology

A Protective Function of IL-22BP in Ischemia Reperfusion and Acetaminophen-Induced Liver Injury

Dörte Kleinschmidt, Anastasios D. Giannou, Heather M. McGee, Jan Kempski, Babett Steglich, Francis Jessica Huber, Thomas Michael Ernst, Ahmad Mustafa Shiri, Claudia Wegscheid, Elena Tasika, Peter Hübener, Philipp Huber, Tanja Bedke, Niklas Steffens, Theodora Agalioti, Tobias Fuchs, Jill Noll, Hannelore Lotter, Gisa Tiegs, Ansgar W. Lohse, Jonathan H. Axelrod, Eithan Galun, Richard A. Flavell, Nicola Gagliani and Samuel Huber

J Immunol 2017; 199:4078-4090; Prepublished online 6 November 2017;
doi: 10.4049/jimmunol.1700587
http://www.jimmunol.org/content/199/12/4078

The Journal of Immunology is published twice each month by
The American Association of Immunologists, Inc.,
1451 Rockville Pike, Suite 650, Rockville, MD 20852

Print ISSN: 0022-1767 Online ISSN: 1550-6606.

A Protective Function of IL-22BP in Ischemia Reperfusion and Acetaminophen-Induced Liver Injury

Dörte Kleinschmidt,*,[1] Anastasios D. Giannou,*,[1] Heather M. McGee,[†] Jan Kempski,* Babett Steglich,*,[‡] Francis Jessica Huber,* Thomas Michael Ernst,[§] Ahmad Mustafa Shiri,* Claudia Wegscheid,[¶] Elena Tasika,[¶] Peter Hübener,* Philipp Huber,* Tanja Bedke,* Niklas Steffens,* Theodora Agalioti,[‡] Tobias Fuchs,[‖] Jill Noll,[#] Hannelore Lotter,[#] Gisa Tiegs,[¶] Ansgar W. Lohse,* Jonathan H. Axelrod, Eithan Galun,** Richard A. Flavell,[††,‡‡] Nicola Gagliani,*,[‡,§§] and Samuel Huber***

Acute liver injury can be secondary to a variety of causes, including infections, intoxication, and ischemia. All of these insults induce hepatocyte death and subsequent inflammation, which can make acute liver injury a life-threatening event. IL-22 is a dual natured cytokine which has context-dependent protective and pathogenic properties during tissue damage. Accordingly, IL-22 was shown to promote liver regeneration upon acute liver damage. However, other studies suggest pathogenic properties of IL-22 during chronic liver injury. IL-22 binding protein (IL-22BP, IL-22Ra2) is a soluble inhibitor of IL-22 that regulates IL-22 activity. However, the significance of endogenous IL-22BP in acute liver injury is unknown. We hypothesized that IL-22BP may play a role in acute liver injury. To test this hypothesis, we used *Il22bp*-deficient mice and murine models of acute liver damage induced by ischemia reperfusion and *N*-acetyl-*p*-aminophenol (acetaminophen) administration. We found that *Il22bp*-deficient mice were more susceptible to acute liver damage in both models. We used *Il22* × *Il22bp* double-deficient mice to show that this effect is indeed due to uncontrolled IL-22 activity. We could demonstrate mechanistically increased expression of *Cxcl10* by hepatocytes, and consequently increased infiltration of inflammatory CD11b$^+$Ly6C$^+$ monocytes into the liver in *Il22bp*-deficient mice upon liver damage. Accordingly, neutralization of CXCL10 reversed the increased disease susceptibility of *Il22bp*-deficient mice. In conclusion, our data indicate that IL-22BP plays a protective role in acute liver damage, via controlling IL-22–induced *Cxcl10* expression. *The Journal of Immunology*, 2017, 199: 4078–4090.

Acute liver failure (ALF) is characterized by loss of hepatic parenchyma and subsequent dysregulation of the liver's metabolic and synthetic functions. Drugs, viruses, toxins, autoimmune diseases, metabolic diseases, and vascular disorders all induce hepatocyte death, and the subsequent inflammatory response contributes to the pathogenesis of ALF. The initial insult to the liver leads to cytokine production, chemokine release, and subsequent infiltration of inflammatory cells into the liver. Clinical outcomes in ALF often correlate with patients' immune response to liver injury as opposed to the extent of the liver injury itself (1). Therefore, tight regulation of the immune response is critical to orchestrate liver regeneration and restore hepatic function, while avoiding excessive inflammation that causes continued liver damage. Despite the severity of this clinical problem, very little is known about the molecular and cellular mechanisms that regulate inflammation and tissue repair during acute liver damage.

IL-22 is a member of the IL-10 cytokine family that plays a key role in signaling between the immune system and the peripheral tissues. Several cell types including Th17, Th22, TCRγδ, NK, NKT, innate lymphoid, and lymphoid-tissue inducer cells can produce IL-22 (2, 3). IL-22 acts via binding to the heterodimer IL-10R2/IL-22R1 complex. IL-22R1 is expressed on nonhematopoietic

*I. Department of Medicine, University Medical Center Hamburg-Eppendorf, 20246 Hamburg, Germany; [†]Department of Radiation Oncology, Icahn School of Medicine at Mount Sinai, New York, NY 10029; [‡]Department of General, Visceral and Thoracic Surgery, University Medical Center Hamburg-Eppendorf, 20246 Hamburg, Germany; [§]Department and Clinic for Diagnostic and Interventional Radiology and Nuclear Medicine, University Medical Center Hamburg-Eppendorf, 20246 Hamburg, Germany; [¶]Institute of Experimental Immunology and Hepatology, University Medical Center Hamburg-Eppendorf, 20246 Hamburg, Germany; [‖]Institute of Clinical Chemistry and Central Laboratories, University Medical Center Hamburg-Eppendorf, 20246 Hamburg, Germany; [#]Bernhard Nocht Institute for Tropical Medicine, 20359 Hamburg, Germany; **Goldyne Savad Institute of Gene Therapy, Hadassah Hebrew University Hospital, Jerusalem 91120, Israel; [††]Department of Immunobiology, School of Medicine, Yale University, New Haven, CT 06520; [‡‡]Howard Hughes Medical Institute, Yale University School of Medicine, New Haven, CT 06520; and [§§]Immunology and Allergy Unit, Department of Medicine Solna, Karolinska Institute, 17176 Stockholm, Sweden

[1]D.K. and A.D.G. contributed equally to this work.

ORCIDs: 0000-0001-8867-5077 (J.K.); 0000-0002-2170-9241 (T.M.E.); 0000-0001-9905-6386 (C.W.); 0000-0002-3244-2300 (P. Huber); 0000-0001-8635-3445 (J.N.); 0000-0003-4461-0778 (R.A.F.).

Received for publication April 26, 2017. Accepted for publication October 7, 2017.

This work was supported by Deutsche Forschungsgemeinschaft Grant SFB841.

D.K. and A.D.G. performed experiments, analyzed the data, and wrote the manuscript; H.M.M. generated the IL-22 reporter mice; J.K. A.M.S., C.W., E.T., P. Huber, N.S., and J.N. performed experiments; B.S. performed the bioinformatics analysis; F.J.H. performed the partial hepatectomy; T.M.E. performed the magnetic resonance imaging; P. Hübener and T.F. assisted with the ischemia reperfusion injury model; T.B., T.A., H.L., G.T., A.W.L., J.H.A., E.G., R.A.F., and N.G. provided material and reagents and made important scientific suggestions; S.H. supervised this study and revised the manuscript.

Address correspondence and reprint requests to Prof. Samuel Huber, I. Department of Medicine, University Medical Center Hamburg-Eppendorf, Martinistrasse 52, 20246 Hamburg, Germany. E-mail address: shuber@uke.de

The online version of this article contains supplemental material.

Abbreviations used in this article: ALF, acute liver failure; ALT, alanine aminotransferase; acetaminophen (APAP), *N*-acetyl-*p*-aminophenol; BP, binding protein; HBV, hepatitis B virus; ILC, innate lymphoid cell; IR, ischemia reperfusion; IRI, IR injury; PHx, partial hepatectomy; rm, recombinant murine.

www.jimmunol.org/cgi/doi/10.4049/jimmunol.1700587

cells, including epithelial cells in the intestine, hepatocytes in the liver, and mesenchymal cells such as fibroblasts in the skin (4). Binding of IL-22 to its receptor complex induces the activation of STAT3, STAT1, and STAT5, as well as the JNKs and MAPKs (5). IL-22 plays an important protective role in tissue regeneration and bacterial infections (6). However, IL-22 can also have pathogenic properties, for example in Th17-driven colitis, rheumatoid arthritis, psoriasis, and selected cancers (7–10). In the liver, IL-22 acts mainly on hepatocytes by inducing the expression of mitogenic and antiapoptotic proteins (11, 12). Furthermore, it induces antioxidant proteins to protect from oxidative stress and acute-phase proteins (13, 14). Hence, IL-22 supports cellular proliferation and therefore enhances liver regeneration (11, 12). IL-22 has been reported to have protective properties upon acute liver damage induced by Con A-, carbon tetrachloride- and ethanol-induced liver injury (15–17). However, there are also studies suggesting that IL-22 might have pathogenic functions in chronic liver damage. Elevated serum levels of IL-22 correlate with a poorer prognosis in patients with hepatitis B virus (HBV) cirrhosis (18, 19). In addition, IL-22 increases chronic liver inflammation by recruiting Th17 cells in HBV-infected patients and HBV-transgenic mice (20, 21).

Taken together, these data suggest context-dependent dual protective and pathogenic properties of IL-22 in the liver, and thus highlight the need of endogenous mechanisms to tightly control the activity of IL-22. IL-22 binding protein (IL-22BP, IL-22Ra2) is a soluble IL-22 receptor that lacks a transmembrane domain and is an endogenous inhibitor of IL-22. Accordingly, it has been shown that IL-22BP binds to IL-22 and blocks the interaction of IL-22 with the membrane-bound IL-22R1 in vitro using human (22, 23) and mouse cells (24, 25). In line with these data, we have shown in mouse models in vivo that the effect of IL-22BP is dependent on the presence of IL-22 (26, 27). These data furthermore suggest that IL-22BP specifically binds to IL-22 also in vivo. Finally, structural analyses and binding assays have shown that IL-22BP has a much higher affinity for IL-22 than it has for the membrane-bound IL-22R1 (28, 29). IL-22BP can be detected in lymphatic organs, the gastrointestinal system, lung, skin, liver, and in the female reproductive system (22, 29). Under steady-state conditions in lymphoid organs and the intestine, IL-22BP is produced by conventional dendritic cells, T cells and eosinophils (27, 30, 31). Accordingly, we and others have shown that endogenous IL-22BP is essential to control IL-22–mediated effects in the intestine (27, 31). Despite these studies, the cellular source and function of endogenous IL-22BP in the liver remain unknown.

In the current study, we used *Il22bp*-deficient mice to analyze the role of IL-22BP during acute liver damage induced by two clinically relevant mouse models, ischemia reperfusion injury (IRI) and *N*-acetyl-*p*-aminophenol (acetaminophen or APAP) intoxication. Liver IRI is a major complication during surgical liver resection and liver transplantation. Ischemic tissue injury is mediated by the generation of reactive oxygen species and immune activation, leading to hepatocellular death (32). APAP-induced liver injury is caused by an overdose of the analgesic and antipyretic drug APAP. The toxic reactive metabolite of APAP is responsible for increased oxidative stress, mitochondrial dysfunction, and necrotic cell death. Using mouse models, we found that *Il22bp*-deficient mice have increased liver injury upon acute liver damage. Using *Il22bp* × *Il22* double-deficient mice we could show that this effect was indeed IL-22 dependent. Mechanistically, we found that IL-22 induced *Cxcl10* expression by hepatocytes and in turn *Il22bp*-deficient mice displayed increased numbers of inflammatory monocytes in the liver. In conclusion, our data indicate a critical function of IL-22BP during acute liver damage.

Materials and Methods

Animals

C57BL/6, $Il22^{-/-}$, $Il22bp^{-/-}$ (26), and $Foxp3^{RFP} \times Il17a^{eGFP} \times Il22^{BFP}$ mice (33–35) were bred and housed under specific pathogen-free conditions in the animal facility of the University Medical Center Hamburg-Eppendorf. Age- and sex-matched littermates between 8 and 16 wk of age were used. Animal experiments were carried out in accordance with the Institutional Review Board "Behörde für Soziales, Familie, Gesundheit und Verbraucherschutz" (Hamburg, Germany).

Mouse liver model of IRI

Mice were anesthetized by isoflurane inhalation and an abdominal incision was performed. An atraumatic clamp was placed across the hepatic artery and portal vein of the middle and left lateral lobe to interrupt the blood supply for 60 min. After removing the clamps, the mice were euthanized at 6, 12, 24, and 48 h after reperfusion. Peripheral serum samples were used for alanine aminotransferase (ALT) level measurement and liver lobes were collected for real-time PCR, RNA sequencing, and immunohistochemical analysis. To study the role of IL-22 or CXCL10, animals were i.p. treated with recombinant murine (rm) IL-22 (5 μg in 200 μl PBS; PeproTech, London, U.K.) 30 min before ischemia or an anti-mouse IL-22 (AF582; 50 μg in 200 μl PBS; R&D Systems, Minneapolis, MN) or an anti-mouse CXCL10 Ab 24 h before ischemia (5 mg/kg; R&D Systems).

APAP intoxication

APAP 350 mg/kg body weight (Sigma-Aldrich, St. Louis, MO) was injected i.p. Liver tissue and blood samples were collected at 6, 24, and 48 h after APAP injection. Mice were fasted for 12–15 h prior to APAP injection.

Partial hepatectomy

Mice were anesthetized using isoflurane inhalation and received carprofen (5 mg/kg) s.c. for analgesia. After a midline laparotomy, the median and left lateral lobe of the liver were ligated around the base and resected to perform a 2/3 partial hepatectomy (PHx). The abdominal wall and skin were sutured separately. After completion of the operation, we maintained analgesia by daily s.c. injection of carprofen. Hepatic volumes were measured by using a seven Tesla MRI scanner (ClinScan; Bruker BioSpin, Ettlingen, Germany) to assess liver regeneration.

Cell isolation

Mice were euthanized and the liver was perfused with ice-cold PBS via the portal vein and drained by cutting the vena cava. The gall bladder was removed and the liver excised. For nonparenchymal cell isolation, the liver was smashed through a 100-μm cell strainer and a Percoll gradient (GE Healthcare, Little Chalfont, U.K.) was performed.

Analysis of ALT activity

Plasma samples were diluted and ALT enzyme levels analyzed at the Department of Clinical Chemistry (University Medical Center Hamburg-Eppendorf).

RNA isolation and real-time PCR

Total RNA from liver tissues was isolated using Trizol reagent (Applied Biosystems, Foster City, CA). High-Capacity cDNA Reverse Transcription Kit (Applied Biosystems) was used to prepare cDNA. Real-time PCR was performed on a StepOnePlus Real-Time PCR System (Applied Biosystems). The probes (Applied Biosystems) were Mm03024075_m1 Hprt, Mm01226722_g1 Il22, Mm01192969_m1 Il22ra2, Mm01192943_m1 Il22ra1, Mm00445235_m1 Cxcl10, Mm04207460_m1 Cxcl1, Mm00444662_m1 Cxcl11, Mm00445553_m1 Cxcl12, Mm04214185_s1 Cxcl13, Mm00441242_m1 Ccl2, Mm00451315_g1 Cxcl4, Mm00436451_g1 Cxcl5, Mm00470163_m1 Cxcl7, Mm00443113_m1 Ccl7.

Fluorescent activated cell sorting

Fc-γ receptors were blocked using a mAb (clone 2.4G2). The cells were stained with fluorochrome-conjugated Abs (Ly6G clone 1A8, Ly6C clone AL-21, CD45.2 clone 104, CD11c clone HL3; BD Pharmingen; CD11b clone M1/70, NK1.1 clone PK136, CD3 clone 17A2, CD4 clone GK1.5, TCRγδ clone GL3, CD5 clone 53-7.3, CD19 clone 6D5, CD4 clone RM4-5; BioLegend; CD49b clone HMα2, TCRβ clone H57-597, CD8 clone 53-6.7, GR1 clone RB6-8C5; eBioscience, San Diego, CA). BD LSRFortessa and FACSAria (BD Biosciences, San Jose, CA) were used for cell analysis and cell sorting, respectively. Data were analyzed using FlowJo v.6.1 (Tree Star, Ashland, OR).

Intracellular cytokine staining

For intracellular cytokine staining, cells were restimulated in DMEM (Life Technologies, Carlsbad, CA) supplemented with 10% FBS (Life Technologies), 1% penicillin/streptomycin (Life Technologies) with PMA (500 ng/ml) (Merck), ionomycin (500 ng/ml) (Sigma-Aldrich) and monensin (2 μM) (BioLegend) for 3 h at 37˚C. After stimulation, cells were stained with extracellular markers, fixed with 4% formaldehyde solution (Sigma-Aldrich) and permeabilized with 0.1% NP-40 (Sigma-Aldrich). Subsequently, the cells were stained with fluorochrome-conjugated Abs (Tbet clone 4B10, IFN-γ clone XMG1.2, IL-17A clone TC11-18H10.1, RORγt clone Q31-378, GATA3 clone L50-832; BD Pharmingen; IL-22 clone 1H8PWSR; eBioscience).

Immunoblotting

To analyze STAT3 activation and CYP2E1 expression, total liver or hepatocyte lysates were separated in a 10% SDS-PAGE assay, transferred to polyvinylidene difluoride membranes (Merck Millipore), probed with anti-phospho-Stat3 (Tyr705), anti-STAT3 Ab (Cell Signaling), anti-CYP2E1 (Merck Millipore) and anti-GAPDH (Santa Cruz Biotechnology) Ab, followed by incubation with the appropriate HRP-conjugated secondary Abs (Dako, Carpintera, CA) and were visualized with the ECL substrate (Merck Millipore).

H&E staining

Liver specimens were fixed in 4% buffered formalin, and embedded in paraffin or OCT (Sakura, Tokyo, Japan) and stored at −80˚C. Tissue sections (4 μm) were prepared and stained with H&E. Necrotic areas were quantified by area fraction analysis (ImageJ, U.S. National Institutes of Health, Bethesda, MD).

Immunohistochemical analysis of Ki-67

Formalin-fixed and paraffin-embedded liver sections were deparaffinized in xylene and graded alcohol solutions, hydrated, and then washed in a PBS. Sections were heat-treated in a microwave oven with 10 mM sodium citrate buffer (pH = 6), then treated with 3% H_2O_2 for 20 min to inhibit endogenous peroxidase and incubated with protein blocking agent 5% FCS/10% BSA in PBS. Slides were then stained with monoclonal Ki-67 Ab (BD Biosciences). For identification of the primary Ab the Envision Detection System-HRP (Dako) was used. Ki-67 expression was further assessed by the image processing program ImageJ.

Detection of in situ cell death using TUNEL assay

Paraffin-embedded liver sections (5 μm) were deparaffinized by soaking twice in xylene for 10 min, then rehydrated by graded washes with ethanol. After treatment with Proteinase K (20 mg/ml) at 37˚C for 30 min, the TUNEL assay was performed in accordance with the manufacturer's instructions (Roche Diagnostic, Basel, Switzerland). The specimens were counterstained with DAPI (Life Technologies) and mounted with ProLong Gold Antifade Mountant. The degree of apoptosis was assessed by point counting using ImageJ.

Isolation of primary hepatocytes

For the isolation of primary hepatocytes, the liver was digested with Liberase (Roche Diagnostics) and the remaining section was gently disrupted to free residual cells. Single-cell suspension was filtered through a 100-μm cell strainer and the cells were allowed to settle by gravity for 20 min. Subsequently, parenchymal cells were separated by 10 min centrifugation in a 90% Percoll gradient (GE Healthcare). For primary hepatocyte culture, William's E + GlutaMAX-I medium (Life Technologies, Karlsruhe, Germany) was supplemented with 10% FBS (Life Technologies), 1% penicillin/streptomycin (Life Technologies) and 1% L-glutamine (Life Technologies). We incubated the cells overnight at 37˚C, 40% O_2. The hepatocytes were washed and treated with 1 ng/ml rmIL-22, rmIL-22BP, or rmIL-6 (eBioscience; R&D Systems; Peprotech, respectively). After 15 or 240 min of incubation, we harvested the cells and extracted RNA and protein.

Immunofluorescence

Liver tissue sections were fixed for 10 min in 4% paraformaldehyde at room temperature. Sections (5 μm) were washed with PBS and incubated in PBS-Triton 0.3% for 5 min. After washing, they were incubated for 60 min in blocking buffer. Samples were stained overnight with chicken anti-LacZ Ab (primary chicken anti-LacZ Ab, 1:100; Abcam) at 4˚C. After washing secondary Ab (Alexa Fluor 488 goat anti-chicken IgG; Invitrogen) staining was performed (1 h, room temperature) followed by 5 min staining with Hoechst 33258 (1:5000). As control, the primary Ab was omitted.

RNA sequencing

Using 2 μg of RNA per sample, sequencing libraries were generated using NEBNext UltraTM RNA Library Prep Kit for Illumina (New England Biolabs). cDNA libraries were sequenced on Illumina HiSEquation 2500 yielding ∼15 million 50 bp single end reads per sample. Overall quality was assessed with FastQC v. 0.11.5 (http://www.bioinformatics.babraham.ac.uk/projects/fastqc/), low quality bases were trimmed off with Trimmomatic (36) v. 0.33, followed by alignment to the *Mus musculus* genome draft GRCm38.84 using STAR (37) v. 2.5.0. For visualization and hierarchical clustering, reads were normalized using the transcripts per million method (38), but raw read counts were used for differential expression analysis using DESeq2 (39) v. 1.14. We observed reads originating from the transgenic constructs used to knock out the *Il22bp* gene, both from the LacZ and neoR genes used for the knockout, as well as from the 3′ UTR. We assume that these are either due to increased mRNA stability caused by the presence of the transgenes, or due to changes in local chromatin structure affecting the base level of transcription from the endogenous promoter. We did not observe any reads originating from the protein coding exons of *Il22bp* in the respective knockout samples. RNA sequencing data are available at the Gene Expression Omnibus (GEO: GSE93034 https://www.ncbi.nlm.nih.gov/geo/).

Statistical analysis

Statistical analysis was performed using GraphPad Prism Software (GraphPad Software, San Diego, CA). For comparison of groups, the nonparametric two-sided Mann–Whitney or Student *t* test were used. Bonferroni correction was used to adjust the *p* value in case of multiple comparisons. For time-dependent liver regeneration data, a repeated-measures ANOVA to assess the significance of the main effects and an experimental group-time interaction was used. The Pearson correlation was used for correlative analyses. The significance level for all analyses was set to $p < 0.05$.

Results

Il22bp-*deficient mice are highly susceptible to hepatic IRI*

IL-22BP is known to inhibit IL-22 in other tissues such as the colon, but the cellular source and function of endogenous IL-22BP in the liver is unknown. We hypothesized that IL-22BP controls the effects of IL-22 during liver regeneration upon acute liver damage (Fig. 1A). To test this hypothesis, we first analyzed the expression pattern of *Il22* and *Il22bp* in wild-type mice during ischemia reperfusion (IR)-induced liver damage by real-time PCR (Fig. 1B). *Il22* mRNA increased in total liver 6 h after IRI, and was still detectable up to 48 h after IRI (Fig. 1B). *Il22bp* mRNA expression was stable during the time period following IR-induced liver injury (Fig. 1B). On the basis of these data, we hypothesized that IL-22BP may play a role for the control of IL-22 activity in this model. To test this hypothesis, we used *Il22*- and *Il22bp*-deficient mice. We measured the level of ALT in the serum and the necrotic area histologically to assess liver damage. Interestingly, *Il22bp*-deficient mice had higher ALT levels and more extensive liver necrosis compared with wild-type mice at 6, 24, and 48 h after IRI (Fig. 1C, 1D). No differences were observed in the ALT level and liver pathology between wild-type and *Il22*-deficient mice (Fig. 1C, 1D). Similar to the ALT and histology results in *Il22bp*-deficient mice, TUNEL staining 6 h after reperfusion revealed severe tissue damage and increased cell death in *Il22bp*-deficient mice compared with wild-type mice (Fig. 1E). Thus, our data indicate that endogenous IL-22BP plays a protective role after IRI, suggesting that uncontrolled IL-22 activity may contribute to the pathogenesis of IRI. Interestingly, *Il22bp*-deficient mice showed the strongest difference compared with wild-type mice 48 h upon IRI suggesting that IL-22BP plays a more important role during tissue repair after injury. *Il22*-deficient mice on the contrary did not show an altered disease severity, suggesting that endogenous IL-22BP might be sufficient to control IL-22

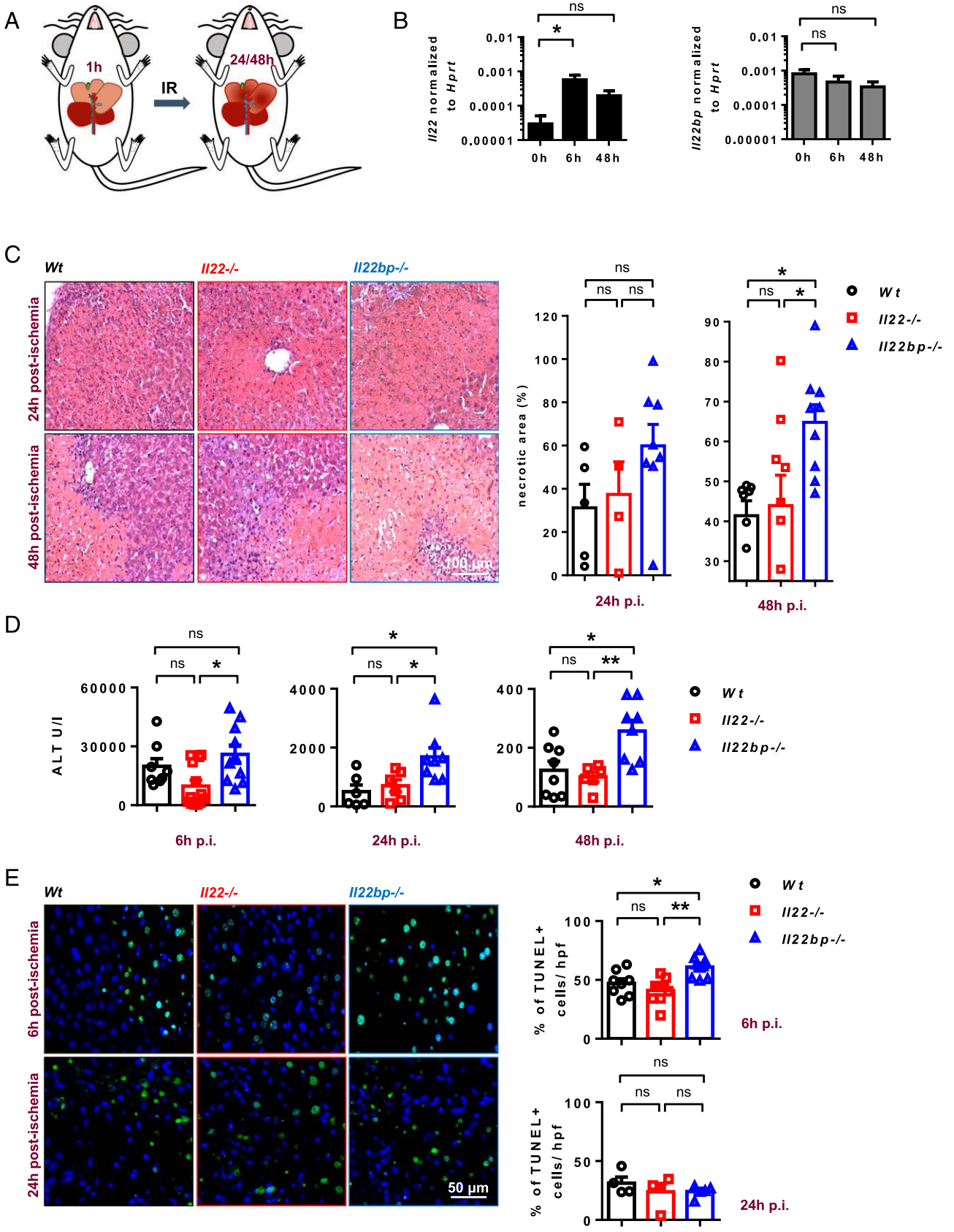

FIGURE 1. Increased liver damage in *Il22bp*$^{-/-}$ mice upon IRI. (**A**) IRI was induced in mice via ligation of the hepatic artery. (**B**) *Il22* and *Il22bp* mRNA (normalized to *Hprt*) in total liver from wild-type (*Wt*) mice ($n = 5$). (**C**) Representative images of H&E stained liver sections from *Wt*, *Il22*$^{-/-}$, and *Il22bp*$^{-/-}$ mice 24 and 48 h after IR. Scale bars = 100 µm. The size of the necrotic areas was evaluated in ImageJ ($n = 4$–10). (**D**) Evaluation of IR-induced liver damage using serum ALT levels at the indicated time points (6, 24, and 48 h) ($n = 6$–10). (**E**) Representative TUNEL staining and statistical analysis of TUNEL-positive liver cells per high power field of vision 6 and 24 h after IRI ($n = 4$–9). Scale bars = 100 µm. Each dot represents one mouse. Data are presented as mean ± SEM. *$p < 0.05$, **$p < 0.01$ as assessed by one-way ANOVA with Bonferroni post hoc tests.

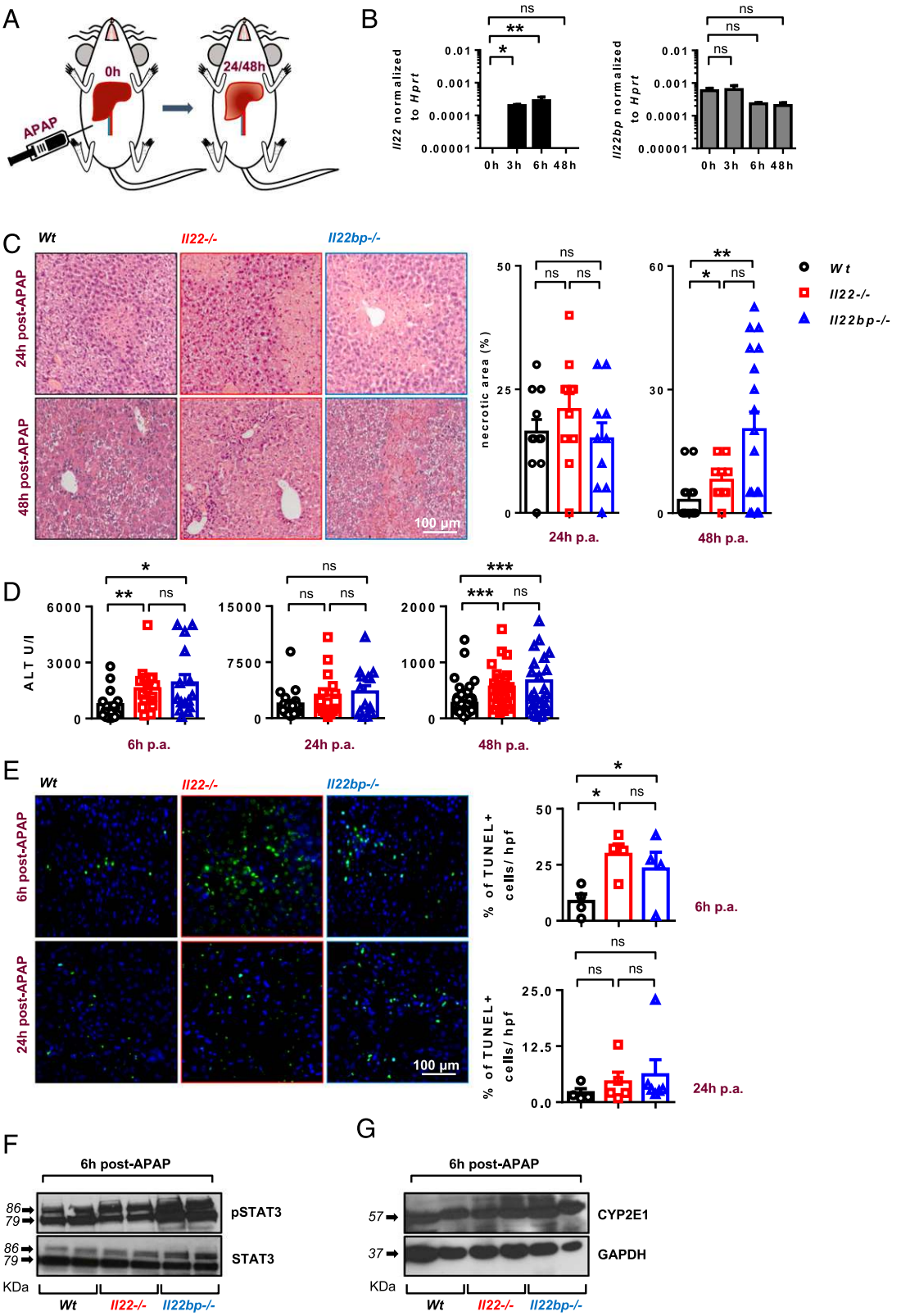

FIGURE 2. *Il22bp*$^{-/-}$ mice are more susceptible to APAP intoxication. (**A**) Acute liver damage was induced via injection of mice with APAP. (**B**) Hepatic *Il22* and *Il22bp* mRNA expression from *Wt* mice ($n = 5$). (**C**) Representative H&E stained liver sections from *Wt*, *Il22*$^{-/-}$, and *Il22bp*$^{-/-}$ mice 24 and 48 h after the onset of APAP intoxication. Scale bars = 100 μm. The size of the necrotic areas was evaluated in ImageJ ($n = 9$–18) (**D**) Evaluation of APAP-induced liver damage using serum ALT levels at the indicated time points (6, 24, and 48 h) ($n = 15$–35). (**E**) Representative TUNEL staining and statistical analysis of TUNEL-positive liver cells per high power field of vision 6 and 24 h after APAP administration ($n = 5$). Scale bars = 100 μm. (**F** and **G**) pSTAT3 and CYP2E1 protein expression relative to STAT3 and GAPDH, respectively, by immunoblotting. Each dot represents one mouse. Data are presented as mean ± SEM. *$p < 0.05$, **$p < 0.01$, ***$p < 0.001$ as assessed by one-way ANOVA with Bonferroni post hoc tests.

activity in wild-type mice in this model. An alternative explanation would be that IL-22BP would have IL-22–independent effects. In order to investigate if the effect observed in *Il22bp*-deficient mice was indeed IL-22 dependent, we performed several experiments. We confirmed that rmIL-22BP is able to block IL-22–mediated STAT3 activation in hepatocytes in vitro (Supplemental Fig. 1A, 1B). We furthermore analyzed ALT levels and the extent of necrosis after IRI in *Il22* × *Il22bp* double-deficient mice in comparison with *Il22*-deficient mice and in *Il22bp*-deficient mice in comparison with wild-type mice in which we blocked IL-22 using a neutralizing Ab. In an IL-22–free environment, *Il22bp*-deficient and *Il22bp*-sufficient mice showed a comparable liver damage, indicating that the effect of IL-22BP is dependent on the presence of IL-22 (Supplemental Fig. 1C, 1D).

Il22bp-*deficient mice show exacerbated liver damage upon APAP administration*

To further confirm a role of IL-22BP during acute liver damage, we used a murine model of drug-induced liver damage and treated mice with a single dose of the analgesic and antipyretic drug APAP (Fig. 2A). We first analyzed the expression pattern of IL-22 and IL-22BP in wild-type mice during APAP-induced liver damage by real-time PCR (Fig. 2B). *Il22* mRNA expression was induced 3 h after APAP exposure and peaked 6 h after treatment. *Il22bp* mRNA expression did not significantly change during the time period following APAP injection (Fig. 2B). To study the role of IL-22BP in liver injury, we injected APAP into both wild-type and *Il22bp*-deficient mice. *Il22bp*-deficient mice were more susceptible to APAP-induced liver damage just as they had been more susceptible to IRI (Fig. 2C). Injection of APAP resulted in significantly higher serum ALT levels in *Il22bp*-deficient mice compared with wild-type mice (Fig. 2D). TUNEL assay demonstrated increased hepatocyte apoptosis in *Il22bp*-deficient mice compared with wild-type mice (Fig. 2E). Interestingly, we found by trend increased CYP2E1 expression in *Il22bp*-deficient mice (Fig. 2F, 2G), which is in line with their significantly enhanced disease severity. Furthermore, APAP administration to *Il22*-deficient mice led to increased histological liver pathology and elevated serum ALT levels. In conclusion, these results suggest that IL-22 has dual functions during APAP-induced liver damage, and highlight the need to control its activity via IL-22BP. However, further studies are needed to test if IL-22BP also plays a protective role in other models of acute liver inflammation, such as Con A-induced hepatitis.

Liver regeneration after PHx is not altered in Il22bp-*deficient mice*

Next, we wanted to assess the role of IL-22BP in another model of liver regeneration, which lacks the presence of necrotic liver tissue and overt inflammation that characterize IR- and APAP-induced liver injury. To that end, we performed PHx (Supplemental Fig. 2A). *Il22* expression was detectable 3 d after PHx and *Il22bp* expression did not change significantly upon PHx (Supplemental Fig. 2B). Livers of wild-type and *Il22bp*-deficient mice reached their original volume 6 d after PHx as assessed by MRI. No difference in regeneration of hepatic mass between wild-type and *Il22bp*-deficient mice was observed (Supplemental Fig. 2C). Analysis of liver sections showed normal histology 6 d after PHx in wild-type and *Il22bp*-deficient mice (Supplemental Fig. 2D). Immunohistochemical staining indicated that the proportion of Ki-67 positive hepatocytes in *Il22bp*-deficient mice was not significantly altered compared with wild-type mice at both 3 and 6 d after PHx. Taken together, these findings show that IL-22BP does not play a significant role during liver regeneration after PHx. Furthermore, these data suggest that the inflammatory response to necrotic cells might be linked to the protective role of IL-22BP in the liver.

CD11b$^+$Ly6C$^+$ cell infiltration in the liver of Il22bp-*deficient mice after IRI*

To characterize the inflammatory environment after acute liver damage, we next analyzed intrahepatic immune cell infiltration by flow cytometry. For these experiments, we focused on the IR-induced liver damage. Interestingly, we found a significant increase of CD11b$^+$Ly6C$^+$ and CD11b$^+$CD11c$^+$ cells in *Il22bp*-deficient mice in comparison with wild-type mice following IRI (Fig. 3C, 3D), whereas other cell populations remained unchanged. Just as wild-type and *Il22*-deficient mice showed similar disease severity after IRI, they showed no differences in the immune cell composition in the liver (Fig. 3A, 3B, 3E–J).

Next, we wanted to assess if the increased frequency of CD11b$^+$ Ly6C$^+$ and CD11b$^+$CD11c$^+$ cells contributes to the expression of IL-22 and IL-22BP in the liver after IRI (Fig. 4A). To answer this question using immunohistochemical techniques, we used heterozygous mice carrying a *LacZ* reporter gene instead of *Il22* or *Il22bp*. *LacZ* expression was used to localize IL-22– and IL-22BP–expressing cells in the liver. As shown in Fig. 4B, β-Galactosidase activity was detected in infiltrating mononuclear cells in the livers of heterozygous *Il22*$^{LacZ+/-}$ and *Il22bp*$^{LacZ+/-}$ mice. To further characterize the cellular source of IL-22 and IL-22BP under steady-state conditions and after IRI, we used real-time PCR and flow cytometry (Fig. 4, Supplemental Fig. 3A, 3B). Interestingly, CD11b$^+$Ly6G$^+$ cells showed the highest expression of *Il22bp* in the liver under steady-state conditions compared with other hematopoietic cell populations. *Il22bp* was highly expressed by CD11b$^+$Ly6G$^+$ cells and induced in CD4$^+$ T cells and CD11b$^+$ Ly6C$^+$ cells 12 h after IRI. As for IL-22, the highest *Il22* expression was detected in CD4$^+$ and CD8$^+$ T cells in steady state. However, *Il22* was strongly expressed in CD11b$^+$Ly6G$^+$ and CD11b$^+$Ly6C$^+$ cells upon IRI (Fig. 4C). Using IL-22 reporter mice, we confirmed that CD11b$^+$Ly6C$^+$ and CD11b$^+$Ly6G$^+$ cells express IL-22 upon IRI (Fig. 4D). Furthermore, it is known that innate lymphoid cells (ILCs) can produce IL-22 and are involved in inflammation and liver regeneration (40). Therefore, we also analyzed ILCs by flow cytometry. No significant numbers of ILC1 were detectable in the liver after IRI. A total of 10% of ILC2 and 44% of ILC3 expressed IL-22 after IRI as opposed to a lower IL-22 expression in the steady-state conditions (Supplemental Fig. 3C–E). However, lineage positive cells (non-ILC) produced the vast majority of IL-22 (Supplemental Fig. 3C–E). In conclusion, IL-22 and IL-22BP are produced by several cell types after IRI. However, we found the strongest upregulation of *Il22* in the CD11b$^+$Ly6C$^+$ cells infiltrating the liver after IRI. *Il22bp* expression was highest in both CD11b$^+$ Ly6G$^+$ and CD11b$^+$Ly6C$^+$ cells in the liver in steady state and after IRI.

Increased Cxcl10 expression in Il22bp-*deficient mice promotes tissue damage during IRI*

To identify the mechanism responsible for the increased tissue damage in livers of *Il22bp*-deficient mice in IRI, we used an unbiased approach using RNA sequencing. We sequenced RNA from liver tissue after IRI and after sham operation from wild-type and *Il22bp*-deficient mice 12 h upon IRI (Fig. 5A). Hierarchical clustering of expression patterns revealed a clear separation between IRI and sham-operated mice (Fig. 5B). Focusing on IRI-treated mice, we found 1307 genes differentially expressed between *Il22bp*-deficient and wild-type mice (Fig. 5C). However, *Il22bp*-deficient mice showed more pronounced liver damage.

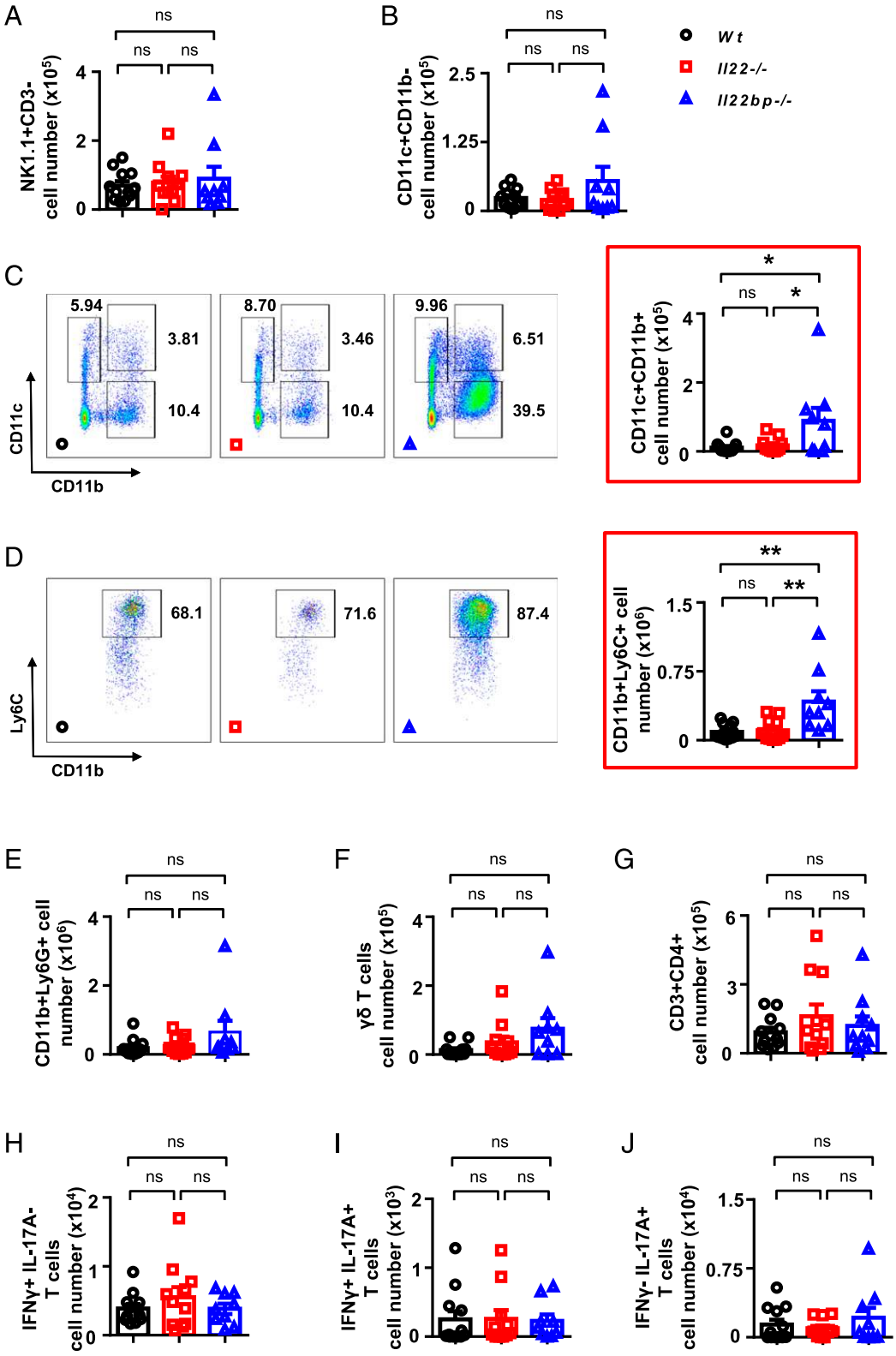

FIGURE 3. CD11b$^+$CD11c$^+$ and CD11b$^+$Ly6C^{high} cells increase in *Il22bp*$^{-/-}$ mice 12 h after IRI. Flow cytometry analysis of liver-infiltrating (**A**) NK1.1$^+$CD3$^+$, (**B**) CD11c$^+$CD11b$^-$, (**C**) CD11b$^+$CD11c$^+$, (**D**) CD11b$^+$Ly6C$^+$, (**E**) CD11b$^+$Ly6G$^+$, (**F**) γδTCR$^+$, (**G**) CD3$^+$CD4$^+$, (**H**) IFN-γ$^+$IL-17$^-$CD3$^+$, (**I**) IFN-γ$^+$IL-17$^+$CD3$^+$, (**J**) IL-17$^+$IFN-γ$^-$CD3$^+$ cells in *Wt*, *Il22*$^{-/-}$, and *Il22bp*$^{-/-}$ mice 12 h after IRI (n = 9–12). Each dot represents one mouse. Data are presented as mean ± SEM. A detailed gating strategy is shown in Supplemental Fig. 3. *$p < 0.05$, **$p < 0.01$ as assessed by one-way ANOVA with Bonferroni post hoc tests.

Thus, it was unclear which of these genes were merely changed because of differences in disease severity. To overcome this caveat, we compared all IRI samples with all control samples. Out of these genes, which were differentially regulated between wild-type and *Il22bp*-deficient mice upon IRI, 348 genes (marked red in Fig. 5C) showed the same change in expression when comparing

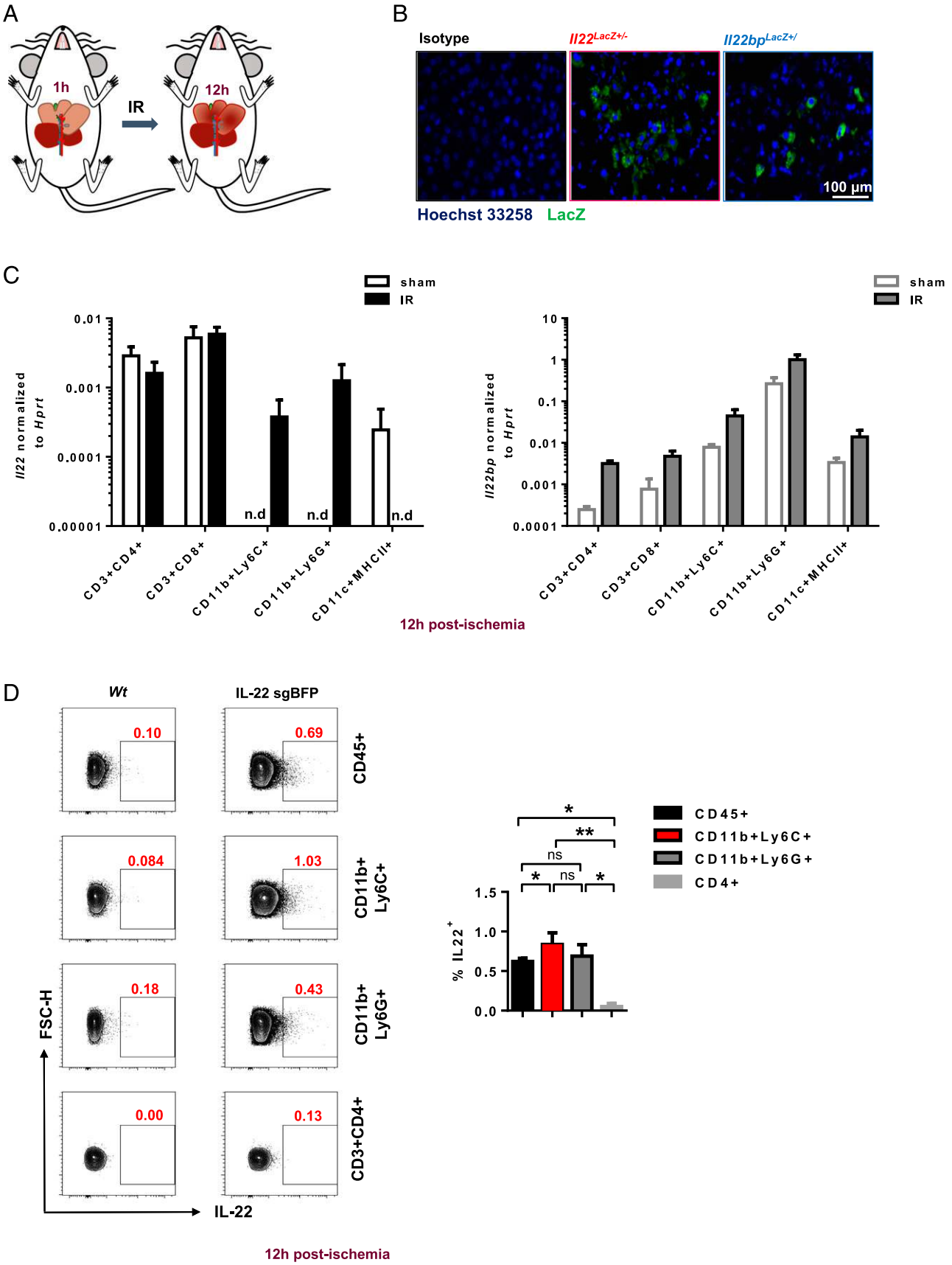

FIGURE 4. IL-22 and IL-22BP expression in liver-infiltrating immune cells after IRI. (**A**) Experimental layout. (**B**) LacZ staining of liver sections from heterozygous *Il22*$^{LacZ+/-}$ and *Il22bp*$^{LacZ+/-}$ mice after IRI. (**C**) Left panel, *Il22* mRNA expression in hepatic immune cell populations from *Wt* mice sorted in the steady state and 12 h after IRI. Data are representative of at least two independent experiments. Right panel, *Il22bp* mRNA expression in hepatic immune cell populations from *Wt* mice sorted in the steady state and 12 h after IRI. Data are representative of at least two independent experiments. (**D**) Flow cytometry analysis of hepatic immune cells isolated from IL-22 sgBFP reporter mice 12 h after IRI. Data are presented as mean ± SEM. *$p < 0.05$, **$p < 0.01$ as assessed by one-way ANOVA with Bonferroni post hoc tests.

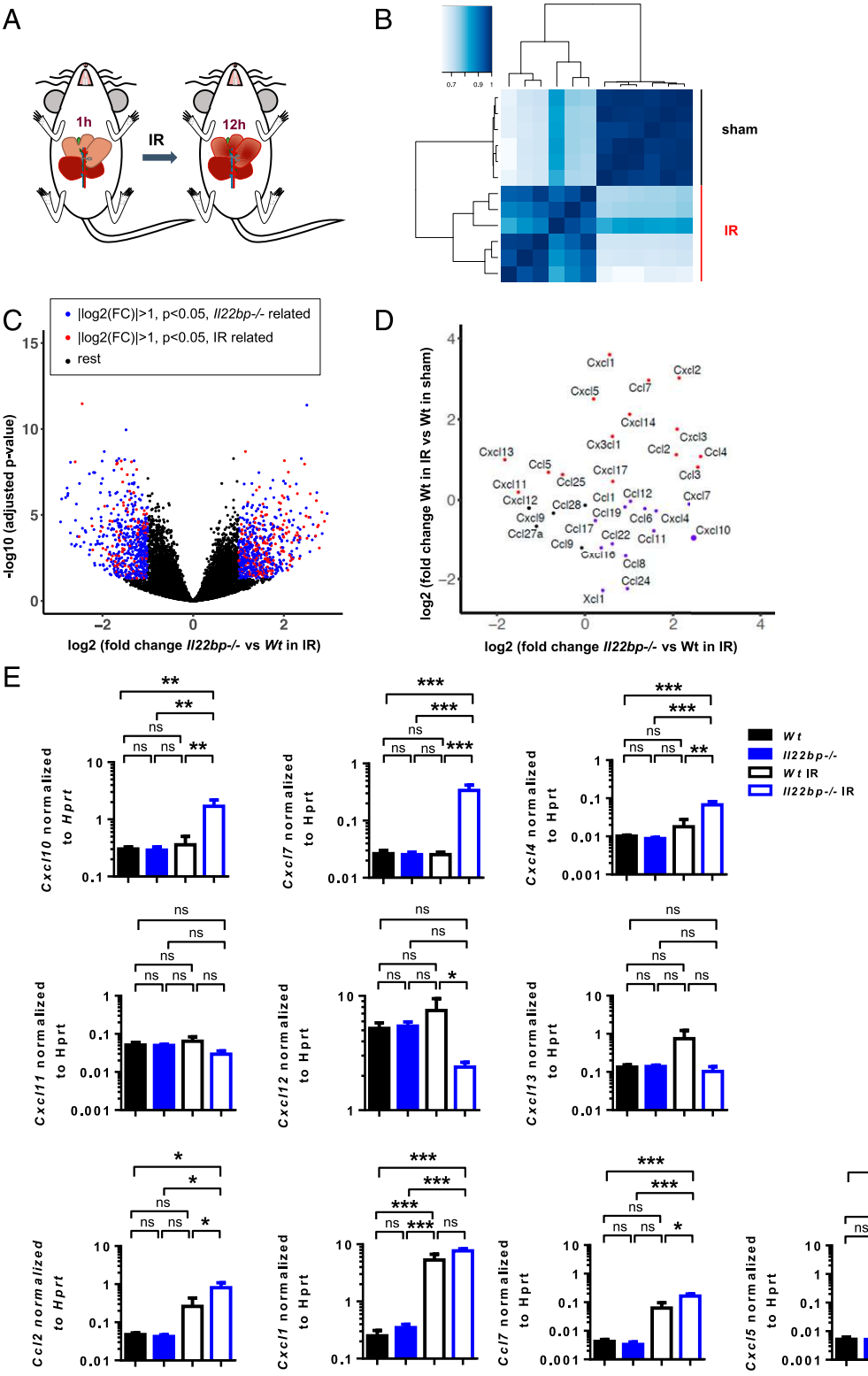

FIGURE 5. *Il22bp* deficiency enhances mRNA expression of the chemokine *Cxcl10* after IRI. (**A**) Experimental layout. (**B**) Hierarchical clustering of RNA sequencing data based on Pearson correlation between transcripts per million normalized read counts of all samples. (**C**) Volcano plot, showing fold change in expression and significance of *Il22bp*$^{-/-}$ versus Wt in IR. Dots in color represent genes with a fold change of at least 2-fold and a p value < 0.05. Red dots mark genes that significantly change their expression in IR in general, whereas blue dots mark genes that specifically change in expression in *Il22bp*$^{-/-}$ versus Wt in IR. Data based on triplicate RNA samples. (**D**) Fold change in chemokine expression, comparing expression changes between *Il22bp*$^{-/-}$ versus Wt after IRI and expression changes between Wt after IRI versus Wt control. Genes colored red show a positive fold change after IRI irrespective of genotype, whereas genes colored blue increase in expression only in *Il22bp*$^{-/-}$ versus Wt. (**E**) Hepatic mRNA expression of *Cxcl10*, *Cxcl7*, *Cxcl4*, *Cxcl11*, *Cxcl12*, *Cxcl13*, *Ccl2*, *Cxcl1*, *Ccl7*, and *Cxcl5* was analyzed in *Wt* and *Il22bp*$^{-/-}$ mice in the steady state and 12 h after IRI (n = 6–16). Data are presented as mean ± SEM. *$p < 0.05$, **$p < 0.01$, ***$p < 0.001$ as assessed by one-way ANOVA with Bonferroni post hoc tests.

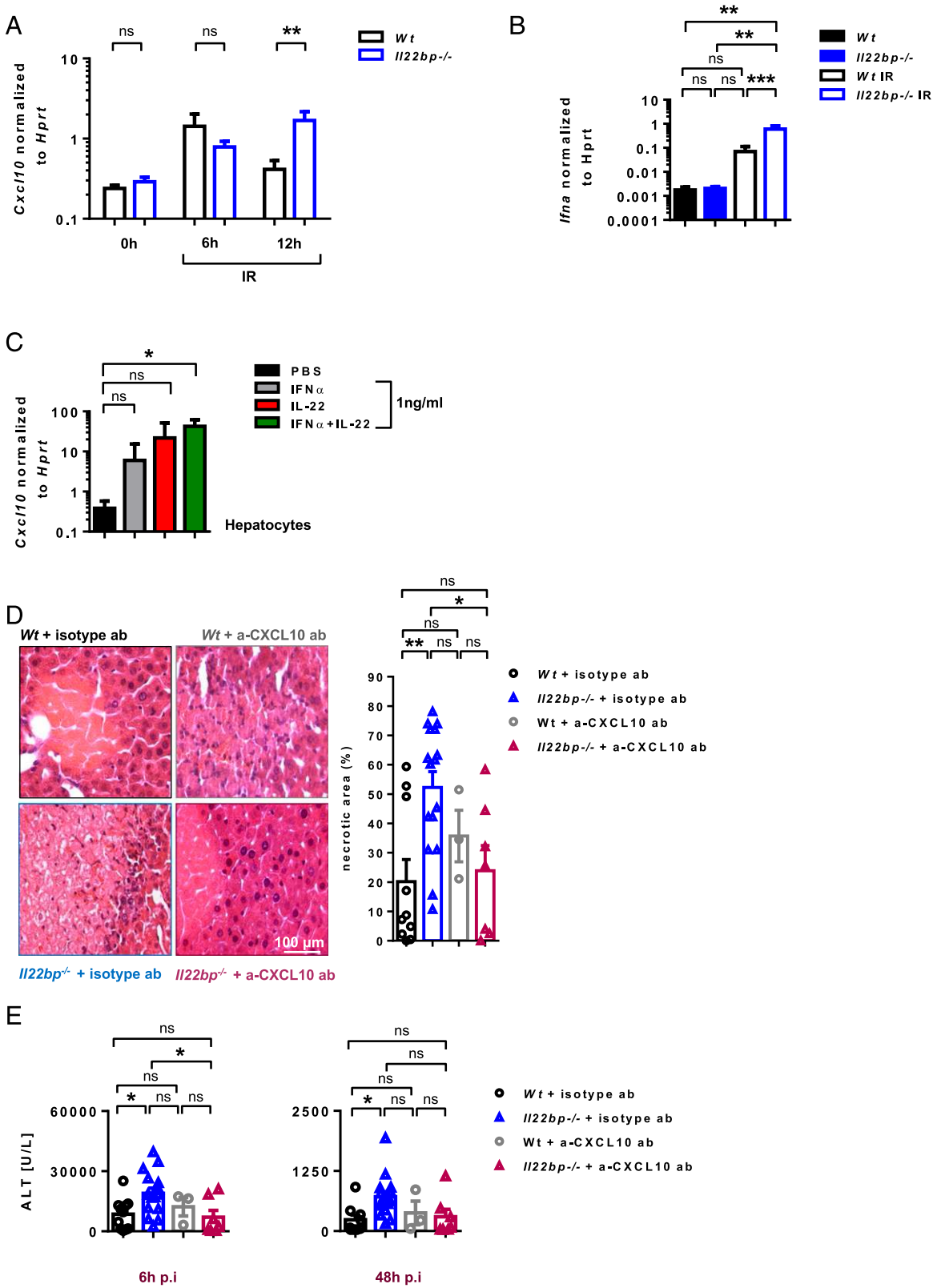

FIGURE 6. Neutralization of Cxcl10 protects *Il22bp*$^{-/-}$ mice against IR-induced liver damage. (**A**) Hepatic mRNA expression of *Cxcl10* was analyzed in *Wt* and *Il22bp*$^{-/-}$ mice in the steady state and 6 and 12 h after IRI (n = 6–16). (**B**) Hepatic mRNA expression of *Ifnα* was analyzed in *Wt* and *Il22bp*$^{-/-}$ mice in the steady state and 12 h after IRI (n = 6–16). (**C**) Real-time PCR analysis of *Cxcl10* expression of primary hepatocytes 4 h after treatment with rmIFN-α, IL-22, or both (1 ng/ml). (**D**) *Wt* and *Il22bp*$^{-/-}$ mice were treated with an anti-CXCL10 (a-CXCL10) Ab 24 h before IR. H&E staining and quantification of necrosis in *Wt* and *Il22bp*$^{-/-}$ mice 48 h post-IR (n = 5–15) (bars = 100 μm). (**E**) Liver damage measured by serum ALT levels at the indicated time points (6 and 48 h). Each dot represents one mouse. Data are presented as mean ± SEM. *$p < 0.05$, **$p < 0.01$, ***$p < 0.001$ as assessed by Student t test [bar graphs in (A)], or by one-way ANOVA with Bonferroni post hoc tests [bar graphs in (D) and (E)].

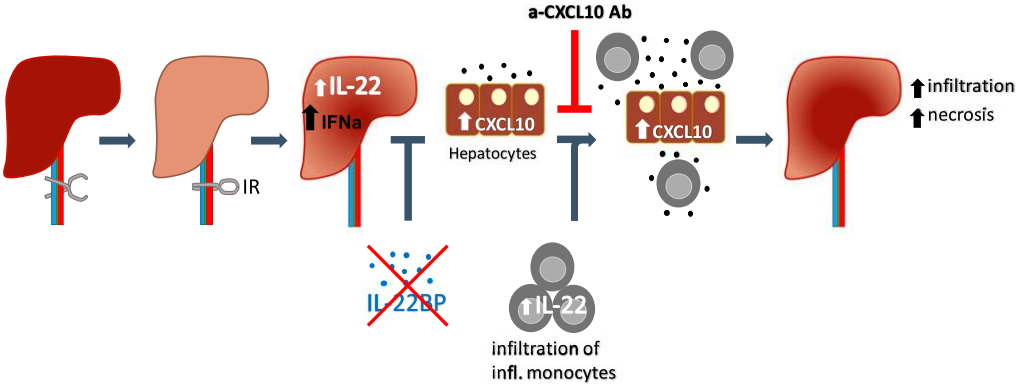

FIGURE 7. Schematic overview of the proposed mechanism.

all IRI samples and all control samples, suggesting they are related to IRI disease severity in general. The remaining 959 genes (marked blue) changed their expression independent of IRI and are therefore affected presumably due to the lack of *Il22bp*. To investigate genes that could be responsible for the increased infiltration of $CD11b^{+}Ly6C^{+}$ cells in the liver of *Il22bp*-deficient mice, we carefully analyzed changes in chemokine expression (Fig. 5D). Although a number of chemokines (marked red) showed increased expression levels in IRI compared with untreated mice, we also observed a group of chemokines (marked blue) that were specifically upregulated only in IRI-treated *Il22bp*-deficient mice compared with IRI-treated wild-type mice, but not in IRI-treated wild-type mice compared with sham-operated wild-type mice. The latter group of chemokines may be involved in mediating the increased disease severity after IRI in *Il22bp*-deficient mice. *Cxcl10* showed the strongest upregulated expression in IRI-treated *Il22bp*-deficient mice compared with IRI-treated wild-type mice, but was moderately downregulated in IRI mice compared with sham-operated wild-type mice. First, we aimed to confirm the difference in *Cxcl10* between wild-type and *Il22bp*-deficient mice upon IRI using real-time PCR. Interestingly, wild-type and *Il22bp*-deficient mice showed a similar *Cxcl10* expression in steady-state conditions. However, *Cxcl10* was significantly upregulated in *Il22bp*-deficient mice but not in wild-type mice after IRI (Fig. 5E). Interestingly, we found that pretreatment of mice with rmIL-22 was protective in the IRI model (Supplemental Fig. 4C). However, *Cxcl10* was not upregulated upon a single injection of rmIL-22 prior to IRI (Supplemental Fig. 4B), whereas we observed prolonged *Cxcl10* expression in *Il22bp*-deficient mice in this model (Fig. 6A). Interestingly, as shown before (41), IFN-α was required for optimal *Cxcl10* induction by IL-22 in vitro (Fig. 6C). Of note, *Ifnα* levels were induced upon IRI but were very low in the liver of healthy mice (Fig. 6B). Therefore, the effect of IL-22 might depend on the time point at which it is present. To investigate if the increased disease susceptibility of *Il22bp*-deficient mice after IRI was Cxcl10 dependent, we blocked Cxcl10 function using a neutralizing Ab. As hypothesized from the expression pattern of *Cxcl10* (Fig. 5E), neutralization of Cxcl10 blocked the increased disease severity after IR-induced tissue damage in *Il22bp*-deficient mice but did not ameliorate disease in wild-type mice (Fig. 6D, 6E). Taken together, these results suggest that uncontrolled IL-22 activity in the presence of IFN-α promotes *Cxcl10* production by hepatocytes after IRI, and this chemokine is responsible for recruiting proinflammatory cells to the damaged liver, which then aggravate liver damage (Fig. 7).

Discussion

IL-22 seems to have context-dependent protective and pathogenic properties during liver damage (42, 43). These studies, however, used *Il22*-deficient mice, systemic blockade of IL-22 using Abs, or transgenic overexpression of IL-22 to elucidate the function of this cytokine (11, 12, 16). One correlative study linked IL-22BP expression in the human liver with liver fibrosis and cirrhosis in humans with chronic liver infections (44). However, functional studies analyzing the role of endogenous IL-22BP, an inhibitor of IL-22 activity, in the liver were missing. Our data indicate a novel and protective function of IL-22BP during acute liver damage. These data are in line with a recent study by Feng et al. (45) who also observed that pretreatment of mice with IL-22 is protective, whereas chronic overexpression of IL-22 (i.e., in IL-22 transgenic mice) worsened disease upon APAP administration. Thus, the IL-22–IL-22BP axis regulates liver regeneration and inflammation upon acute damage.

A tight regulation of the immune response and cytokine production is critical to orchestrate liver regeneration and restore hepatic function. In this study, we focused on the role of IL-22 and IL-22BP during acute liver damage. In line with previous studies (12, 16), we found that hepatic expression of *Il22* is upregulated upon acute liver damage. Previously, we reported that IL-22 and IL-22BP demonstrate an inverse expression pattern compared with IL-22BP during intestinal tissue damage (IL-22 was upregulated, whereas IL-22BP was downregulated) (26). Interestingly, *Il22bp* expression was not changed upon acute liver damage (Fig. 1B), suggesting a different regulation of IL-22BP in the liver compared with the intestine. The downregulation of IL-22BP in the intestine was mediated by the microbiome and inflammasome activation. Thus, the different inflammatory environments in the intestine and the liver may account for these differences. However, also the cellular source of IL-22BP is different in the intestine (27, 30, 31) and the liver. Under steady-state conditions, $CD11b^{+}Ly6G^{+}$ cells showed the highest level of *Il22bp* expression in the liver (Fig. 4C), yet dendritic cells represent the greatest source of IL-22BP in the intestine (26). Dendritic cells, monocytes, and T cells express IL-22BP after liver damage, which is similar to the intestine where dendritic cells, $CD4^{+}$ T cells, and eosinophils express IL-22BP upon tissue damage (26, 30, 31). Taken together, these data show tissue-dependent variations in the regulation and cellular source of IL-22BP.

The hepatoprotective effects of IL-22 are well documented. IL-22 supports cellular proliferation and therefore enhances liver regeneration (11, 12, 43, 46). In line with these data, it was shown that pretreatment of mice with a single dose of IL-22 is beneficial in IRI and APAP-induced liver damage (45, 47, 48) partially because IL-22 stimulates hepatocyte proliferation by activation of

STAT3 (48). Additionally, RORγt$^+$ NK22 cells were reported to play a protective role in IR-induced liver damage (49). These data indicate that IL-22 can perform protective functions during acute liver damage. However, another study showed that neutralization of IL-22 using an Ab did not alter disease severity after IRI liver damage (47). In line with this study, we found that deletion of IL-22 has no significant effect on disease severity and regeneration after IRI liver damage. Of note, IL-22 expression is influenced by the microbiome, and mice housed in our animal facility showed relatively low expression of IL-22 in steady state and upon liver injury. Thus, it would be possible that in wild-type mice the endogenous IL-22BP is sufficient to block IL-22 during IRI liver damage, which might explain why *Il22*-deficient mice do not show a different disease severity compared with wild-type. Furthermore, it was shown that hepatocyte responses to IL-22 stimulation are reduced in hypoxic environments (50), which might further limit the effect of IL-22 in the IRI model. Finally, the observed differences between the above-mentioned studies could be due to different time- and dose-dependent effects of IL-22. This idea would be in line with a study by Feng et al. (45) that showed different acute and chronic effects of IL-22 on APAP-induced liver injury. However, none of the above-mentioned studies analyzed the role of endogenous IL-22BP. We used *Il22bp*-deficient mice to examine the effects of uncontrolled IL-22 activity in mice after IRI and APAP-mediated liver damage. We found that IL-22BP deficiency leads to an exacerbation of DNA damage and cell death after acute liver injury. This effect was indeed dependent on IL-22 as shown by using *Il22* × *Il22bp* double-deficient mice.

Next, we wanted to identify the mechanism by which uncontrolled IL-22 activity promotes liver pathology upon acute liver damage. Interestingly, the increased damage in *Il22bp*-deficient mice was accompanied by a higher infiltration of inflammatory CD11b$^+$Ly6C^{high} monocytes and CD11b$^+$CD11c$^+$ dendritic cells into the liver (Fig. 3C, 3D). Infiltrating monocytes are known to exacerbate liver IRI, but the role of dendritic cells in IRI is still controversial (51–53). We thus wanted to investigate the mechanism linking *Il22bp* deficiency with increased infiltration of the liver with CD11b$^+$Ly6C^{high} monocytes. Using an unbiased approach, we found that several chemokines were upregulated in *Il22bp*-deficient animals upon acute liver damage. We then focused on the role of Cxcl10 because it was shown before that *Cxcl10*-deficient mice are protected against IR-induced liver inflammation and hepatocellular injury (54). Furthermore, IL-22 has been shown before to influence hepatic expression of Cxcl10 in a HBV-transgenic mouse model (20, 21). We therefore tested using a neutralizing Ab, whether the increased disease susceptibility of *Il22bp*-deficient mice was dependent on Cxcl10. Indeed, our data show that blockade of Cxcl10 reversed the increased disease susceptibility of *Il22bp*-deficient mice after acute liver damage (Fig. 6D, 6E). Finally, in line with a previous study which assessed the role of IL-22 in combination with IFN-α on tumor cell lines (41), we showed that IL-22 is able to promote *Cxcl10* expression in primary murine hepatocytes in vitro, albeit at lower levels compared with the in vivo effects. Interestingly, it has been shown by others that injection of healthy mice with rmIL-22 alone does not upregulate *Cxcl10* (55). Accordingly, we found that IFN-α is required for optimal induction of *Cxcl10* by IL-22 (Fig. 6C). Interestingly, *Ifnα* expression was very low in wild-type mice prior to liver damage, but was upregulated upon IRI (Fig. 6B). These data suggest that the effect of IL-22 might depend on the time point at which it is present.

In summary, we found that endogenous IL-22BP has a protective effect upon acute liver damage after IRI and APAP toxicity. Furthermore, *Il22bp*-deficient mice showed increased expression of *Cxcl10* upon liver damage and recruitment of inflammatory monocytes into the liver. Finally, blockade of CXCL10 reversed the increased disease susceptibility of *Il22bp*-deficient mice. These results demonstrate a novel function of IL-22BP to control the pathogenic effects of IL-22 upon acute liver damage.

Acknowledgments

We thank Cathleen Haueis and Sandra Wende for excellent technical assistance. Furthermore, we are grateful to Jan-Eric Turner for assisting us with ILC staining experiments. Cell sorting was performed by the flow cytometry core facility of the University Medical Center Hamburg-Eppendorf. *Il22*-deficient mice (VG1150) and *Il22bp*-deficient mice (VG437) were provided by Regeneron. Dr. Anastasios Giannou is the recipient of a European Respiratory Society Fellowship (STRTF 2015). We are grateful to Prof. Stefan Kurtz at the Center for Bioinformatics of the University of Hamburg for providing access to the high-performance computing cluster.

Disclosures

The authors have no financial conflicts of interest.

References

1. Antoniades, C. G., P. A. Berry, J. A. Wendon, and D. Vergani. 2008. The importance of immune dysfunction in determining outcome in acute liver failure. *J. Hepatol.* 49: 845–861.
2. Witte, E., K. Witte, K. Warszawska, R. Sabat, and K. Wolk. 2010. Interleukin-22: a cytokine produced by T, NK and NKT cell subsets, with importance in the innate immune defense and tissue protection. *Cytokine Growth Factor Rev.* 21: 365–379.
3. Rankin, L. C., M. J. Girard-Madoux, C. Seillet, L. A. Mielke, Y. Kerdiles, A. Fenis, E. Wieduwild, T. Putoczki, S. Mondot, O. Lantz, et al. 2016. Complementarity and redundancy of IL-22-producing innate lymphoid cells. *Nat. Immunol.* 17: 179–186.
4. McGee, H. M., B. A. Schmidt, C. J. Booth, G. D. Yancopoulos, D. M. Valenzuela, A. J. Murphy, S. Stevens, R. A. Flavell, and V. Horsley. 2013. IL-22 promotes fibroblast-mediated wound repair in the skin. *J. Invest. Dermatol.* 133: 1321–1329.
5. Lejeune, D., L. Dumoutier, S. Constantinescu, W. Kruijer, J. J. Schuringa, and J. C. Renauld. 2002. Interleukin-22 (IL-22) activates the JAK/STAT, ERK, JNK, and p38 MAP kinase pathways in a rat hepatoma cell line. Pathways that are shared with and distinct from IL-10. *J. Biol. Chem.* 277: 33676–33682.
6. Sonnenberg, G. F., L. A. Fouser, and D. Artis. 2011. Border patrol: regulation of immunity, inflammation and tissue homeostasis at barrier surfaces by IL-22. *Nat. Immunol.* 12: 383–390.
7. Perusina Lanfranca, M., Y. Lin, J. Fang, W. Zou, and T. Frankel. 2016. Biological and pathological activities of interleukin-22. *J. Mol. Med. (Berl.)* 94: 523–534.
8. Kamanaka, M., S. Huber, L. A. Zenewicz, N. Gagliani, C. Rathinam, W. O'Connor, Jr., Y. Y. Wan, S. Nakae, Y. Iwakura, L. Hao, and R. A. Flavell. 2011. Memory/effector (CD45RB(lo)) CD4 T cells are controlled directly by IL-10 and cause IL-22-dependent intestinal pathology. *J. Exp. Med.* 208: 1027–1040.
9. Zhang, L., J. M. Li, X. G. Liu, D. X. Ma, N. W. Hu, Y. G. Li, W. Li, Y. Hu, S. Yu, X. Qu, et al. 2011. Elevated Th22 cells correlated with Th17 cells in patients with rheumatoid arthritis. *J. Clin. Immunol.* 31: 606–614.
10. Wolk, K., H. S. Haugen, W. Xu, E. Witte, K. Waggie, M. Anderson, E. Vom Baur, K. Witte, K. Warszawska, S. Philipp, et al. 2009. IL-22 and IL-20 are key mediators of the epidermal alterations in psoriasis while IL-17 and IFN-gamma are not. *J. Mol. Med. (Berl.)* 87: 523–536.
11. Park, O., H. Wang, H. Weng, L. Feigenbaum, H. Li, S. Yin, S. H. Ki, S. H. Yoo, S. Dooley, F. S. Wang, et al. 2011. In vivo consequences of liver-specific interleukin-22 expression in mice: Implications for human liver disease progression. *Hepatology* 54: 252–261.
12. Radaeva, S., R. Sun, H. N. Pan, F. Hong, and B. Gao. 2004. Interleukin 22 (IL-22) plays a protective role in T cell-mediated murine hepatitis: IL-22 is a survival factor for hepatocytes via STAT3 activation. *Hepatology* 39: 1332–1342.
13. Dumoutier, L., E. Van Roost, D. Colau, and J. C. Renauld. 2000. Human interleukin-10-related T cell-derived inducible factor: molecular cloning and functional characterization as an hepatocyte-stimulating factor. *Proc. Natl. Acad. Sci. USA* 97: 10144–10149.
14. Liang, S. C., C. Nickerson-Nutter, D. D. Pittman, Y. Carrier, D. G. Goodwin, K. M. Shields, A. J. Lambert, S. H. Schelling, Q. G. Medley, H. L. Ma, et al. 2010. IL-22 induces an acute-phase response. *J. Immunol.* 185: 5531–5538.
15. Ki, S. H., O. Park, M. Zheng, O. Morales-Ibanez, J. K. Kolls, R. Bataller, and B. Gao. 2010. Interleukin-22 treatment ameliorates alcoholic liver injury in a murine model of chronic-binge ethanol feeding: role of signal transducer and activator of transcription 3. *Hepatology* 52: 1291–1300.
16. Zenewicz, L. A., G. D. Yancopoulos, D. M. Valenzuela, A. J. Murphy, M. Karow, and R. A. Flavell. 2007. Interleukin-22 but not interleukin-17 provides protection to hepatocytes during acute liver inflammation. *Immunity* 27: 647–659.

17. Pan, H., F. Hong, S. Radaeva, and B. Gao. 2004. Hydrodynamic gene delivery of interleukin-22 protects the mouse liver from concanavalin A-, carbon tetrachloride-, and Fas ligand-induced injury via activation of STAT3. *Cell. Mol. Immunol.* 1: 43–49.
18. Wu, L.-Y., S. Liu, Y. Liu, C. Guo, H. Li, W. Li, X. Jin, K. Zhang, P. Zhao, L. Wei, and J. Zhao. 2015. Up-regulation of interleukin-22 mediates liver fibrosis via activating hepatic stellate cells in patients with hepatitis C. *Clin. Immunol.* 158: 77–87.
19. Kronenberger, B., I. Rudloff, M. Bachmann, F. Brunner, L. Kapper, N. Filmann, O. Waidmann, E. Herrmann, J. Pfeilschifter, S. Zeuzem, et al. 2012. Interleukin-22 predicts severity and death in advanced liver cirrhosis: a prospective cohort study. *BMC Med.* 10: 102.
20. Zhao, J., Z. Zhang, Y. Luan, Z. Zou, Y. Sun, Y. Li, L. Jin, C. Zhou, J. Fu, B. Gao, et al. 2014. Pathological functions of interleukin-22 in chronic liver inflammation and fibrosis with hepatitis B virus infection by promoting T helper 17 cell recruitment. *Hepatology* 59: 1331–1342.
21. Zhang, Y., M. A. Cobleigh, J. Q. Lian, C. X. Huang, C. J. Booth, X. F. Bai, and M. D. Robek. 2011. A proinflammatory role for interleukin-22 in the immune response to hepatitis B virus. *Gastroenterology* 141: 1897–1906.
22. Dumoutier, L., D. Lejeune, D. Colau, and J. C. Renauld. 2001. Cloning and characterization of IL-22 binding protein, a natural antagonist of IL-10-related T cell-derived inducible factor/IL-22. *J. Immunol.* 166: 7090–7095.
23. Kotenko, S. V., L. S. Izotova, O. V. Mirochnitchenko, E. Esterova, H. Dickensheets, R. P. Donnelly, and S. Pestka. 2001. Identification, cloning, and characterization of a novel soluble receptor that binds IL-22 and neutralizes its activity. *J. Immunol.* 166: 7096–7103.
24. Wei, C. C., T. W. Ho, W. G. Liang, G. Y. Chen, and M. S. Chang. 2003. Cloning and characterization of mouse IL-22 binding protein. *Genes Immun.* 4: 204–211.
25. Weber, G. F., S. Schlautkötter, S. Kaiser-Moore, F. Altmayr, B. Holzmann, and H. Weighardt. 2007. Inhibition of interleukin-22 attenuates bacterial load and organ failure during acute polymicrobial sepsis. *Infect. Immun.* 75: 1690–1697.
26. Huber, S., N. Gagliani, L. A. Zenewicz, F. J. Huber, L. Bosurgi, B. Hu, M. Hedl, W. Zhang, W. O'Connor, Jr., A. J. Murphy, et al. 2012. IL-22BP is regulated by the inflammasome and modulates tumorigenesis in the intestine. *Nature* 491: 259–263.
27. Pelczar, P., M. Witkowski, L. G. Perez, J. Kempski, A. G. Hammel, L. Brockmann, D. Kleinschmidt, S. Wende, C. Haueis, T. Bedke, et al. 2016. A pathogenic role for T cell-derived IL-22BP in inflammatory bowel disease. *Science* 354: 358–362.
28. Jones, B. C., N. J. Logsdon, and M. R. Walter. 2008. Structure of IL-22 bound to its high-affinity IL-22R1 chain. *Structure* 16: 1333–1344.
29. Wolk, K., E. Witte, U. Hoffmann, W. D. Doecke, S. Endesfelder, K. Asadullah, W. Sterry, H. D. Volk, B. M. Wittig, and R. Sabat. 2007. IL-22 induces lipopolysaccharide-binding protein in hepatocytes: a potential systemic role of IL-22 in Crohn's disease. *J. Immunol.* 178: 5973–5981.
30. Martin, J. C., G. Bériou, M. Heslan, C. Chauvin, L. Utriainen, A. Aumeunier, C. L. Scott, A. Mowat, V. Cerovic, S. A. Houston, et al. 2014. Interleukin-22 binding protein (IL-22BP) is constitutively expressed by a subset of conventional dendritic cells and is strongly induced by retinoic acid. *Mucosal Immunol.* 7: 101–113.
31. Martin, J. C., G. Bériou, M. Heslan, C. Bossard, A. Jarry, A. Abidi, P. Hulin, S. Ménoret, R. Thinard, I. Anegon, et al. 2016. IL-22BP is produced by eosinophils in human gut and blocks IL-22 protective actions during colitis. *Mucosal Immunol.* 9: 539–549.
32. Abe, Y., I. N. Hines, G. Zibari, K. Pavlick, L. Gray, Y. Kitagawa, and M. B. Grisham. 2009. Mouse model of liver ischemia and reperfusion injury: method for studying reactive oxygen and nitrogen metabolites in vivo. *Free Radic. Biol. Med.* 46: 1–7.
33. Wan, Y. Y., and R. A. Flavell. 2005. Identifying Foxp3-expressing suppressor T cells with a bicistronic reporter. *Proc. Natl. Acad. Sci. USA* 102: 5126–5131.
34. Huber, S., N. Gagliani, E. Esplugues, W. O'Connor, Jr., F. J. Huber, A. Chaudhry, M. Kamanaka, Y. Kobayashi, C. J. Booth, A. Y. Rudensky, et al. 2011. Th17 cells express interleukin-10 receptor and are controlled by $Foxp3^{-}$ and Foxp3+ regulatory CD4+ T cells in an interleukin-10-dependent manner. *Immunity* 34: 554–565.
35. Esplugues, E., S. Huber, N. Gagliani, A. E. Hauser, T. Town, Y. Y. Wan, W. O'Connor, Jr., A. Rongvaux, N. Van Rooijen, A. M. Haberman, et al. 2011. Control of TH17 cells occurs in the small intestine. *Nature* 475: 514–518.
36. Bolger, A. M., M. Lohse, and B. Usadel. 2014. Trimmomatic: a flexible trimmer for Illumina sequence data. *Bioinformatics* 30: 2114–2120.
37. Dobin, A., C. A. Davis, F. Schlesinger, J. Drenkow, C. Zaleski, S. Jha, P. Batut, M. Chaisson, and T. R. Gingeras. 2013. STAR: ultrafast universal RNA-seq aligner. *Bioinformatics* 29: 15–21.
38. Li, B., and C. N. Dewey. 2011. RSEM: accurate transcript quantification from RNA-Seq data with or without a reference genome. *BMC Bioinformatics* 12: 323.
39. Love, M. I., W. Huber, and S. Anders. 2014. Moderated estimation of fold change and dispersion for RNA-seq data with DESeq2. *Genome Biol.* 15: 550.
40. Kudira, R., T. Malinka, A. Kohler, M. Dosch, M. G. de Agüero, N. Melin, S. Haegele, P. Starlinger, N. Maharjan, S. Saxena, et al. 2016. P2X1-regulated IL-22 secretion by innate lymphoid cells is required for efficient liver regeneration. *Hepatology* 63: 2004–2017.
41. Bachmann, M., S. Ulziibat, L. Härdle, J. Pfeilschifter, and H. Mühl. 2013. IFNα converts IL-22 into a cytokine efficiently activating STAT1 and its downstream targets. *Biochem. Pharmacol.* 85: 396–403.
42. Carmo, R. F., M. S. Cavalcanti, and P. Moura. 2017. Role of Interleukin-22 in chronic liver injury. *Cytokine* 98: 107–114.
43. Sabat, R., W. Ouyang, and K. Wolk. 2014. Therapeutic opportunities of the IL-22-IL-22R1 system. *Nat. Rev. Drug Discov.* 13: 21–38
44. Sertorio, M., X. Hou, R. F. Carmo, H. Dessein, S. Cabantous, M. Abdelwahed, A. Romano, F. Albuquerque, L. Vasconcelos, T. Carmo, et al. 2015. IL-22 and IL-22 binding protein (IL-22BP) regulate fibrosis and cirrhosis in hepatitis C virus and schistosome infections. *Hepatology* 61: 1321–1331
45. Feng, D., Y. Wang, H. Wang, H. Weng, X. Kong, B. V. Martin-Murphy, Y. Li, O. Park, S. Dooley, C. Ju, and B. Gao. 2014. Acute and chronic effects of IL-22 on acetaminophen-induced liver injury. *J. Immunol.* 193: 2512–2518.
46. Feng, D., X. Kong, H. Weng, O. Park, H. Wang, S. Dooley, M. E. Gershwin, and B. Gao. 2012. Interleukin-22 promotes proliferation of liver stem/progenitor cells in mice and patients with chronic hepatitis B virus infection. *Gastroenterology* 143: 188–198.e187.
47. Chestovich, P. J., Y. Uchida, W. Chang, M. Ajalat, C. Lassman, R. Sabat, R. W. Busuttil, and J. W. Kupiec-Weglinski. 2012. Interleukin-22: implications for liver ischemia-reperfusion injury. *Transplantation* 93: 485–492.
48. Scheiermann, P., M. Bachmann, I. Goren, B. Zwissler, J. Pfeilschifter, and H. Mühl. 2013. Application of interleukin-22 mediates protection in experimental acetaminophen-induced acute liver injury. *Am. J. Pathol.* 182: 1107–1113.
49. Eggenhofer, E., M. Sabet-Rashedi, M. Lantow, P. Renner, J. Rovira, G. E. Koehl, H. J. Schlitt, E. K. Geissler, and A. Kroemer. 2016. RORγt(+) IL-22-producing NKp46(+) cells protect from hepatic ischemia reperfusion injury in mice. *J. Hepatol.* 64: 128–134.
50. Budda, S. A., A. Girton, J. G. Henderson, and L. A. Zenewicz. 2016. Transcription factor HIF-1α controls expression of the cytokine IL-22 in CD4 T cells. *J. Immunol.* 197: 2646–2652.
51. Bamboat, Z. M., L. M. Ocuin, V. P. Balachandran, H. Obaid, G. Plitas, and R. P. DeMatteo. 2010. Conventional DCs reduce liver ischemia/reperfusion injury in mice via IL-10 secretion. *J. Clin. Invest.* 120: 559–569.
52. Zhai, Y., R. W. Busuttil, and J. W. Kupiec-Weglinski. 2011. Liver ischemia and reperfusion injury: new insights into mechanisms of innate-adaptive immune-mediated tissue inflammation. *Am. J. Transplant.* 11: 1563–1569.
53. Castellaneta, A., O. Yoshida, S. Kimura, S. Yokota, D. A. Geller, N. Murase, and A. W. Thomson. 2014. Plasmacytoid dendritic cell-derived IFN-α promotes murine liver ischemia/reperfusion injury by induction of hepatocyte IRF-1. *Hepatology* 60: 267–277.
54. Zhai, Y., X. D. Shen, F. Gao, A. Zhao, M. C. Freitas, C. Lassman, A. D. Luster, R. W. Busuttil, and J. W. Kupiec-Weglinski. 2008. CXCL10 regulates liver innate immune response against ischemia and reperfusion injury. *Hepatology* 47: 207–214.
55. Zheng, M., W. Horne, J. P. McAleer, D. Pociask, T. Eddens, M. Good, B. Gao, and J. K. Kolls. 2016. Therapeutic role of interleukin 22 in experimental intra-abdominal *Klebsiella pneumoniae* infection in mice. *Infect. Immun.* 84: 782–789.